Cellular and Molecular Bioengineering (© 2014)
DOI: 10.1007/s12195-014-0353-8

BMES BIOMEDICAL ENGINEERING SOCIETY™ www.bmes.org

Microscale Bioadhesive Hydrogel Arrays for Cell Engineering Applications

RAVI GHANSHYAM PATEL,[1] ALBERTO PURWADA,[2] LEANDRO CERCHIETTI,[3] GIORGIO INGHIRAMI,[4] ARI MELNICK,[3] AKHILESH K. GAHARWAR,[5,6] and ANKUR SINGH[1]

[1]Sibley School of Mechanical and Aerospace Engineering, Cornell University, Ithaca, NY 14853, USA; [2]Department of Biomedical Engineering, Cornell University, Ithaca, NY 14853, USA; [3]Division of Hematology and Medical Oncology, Weill Cornell Medical College, Cornell University, New York, NY 10065, USA; [4]Department of Pathology, Weill Cornell Medical College, Cornell University, New York, NY 10065, USA; [5]Department of Biomedical Engineering, Texas A&M University, College Station, TX 77843, USA; and [6]Department of Materials Science & Engineering, Texas A&M University, College Station, TX 77843, USA

(Received 15 February 2014; accepted 28 July 2014)

Associate Editor David Mooney oversaw the review of this article.

Abstract—Bioengineered hydrogels have been explored in cell and tissue engineering applications to support cell growth and modulate its behavior. A rationally designed scaffold should allow for encapsulated cells to survive, adhere, proliferate, remodel the niche, and can be used for controlled delivery of biomolecules. Here we report a microarray of composite bioadhesive microgels with modular dimensions, tunable mechanical properties and bulk modified adhesive biomolecule composition. Composite bioadhesive microgels of maleimide functionalized polyethylene glycol (PEG-MAL) with interpenetrating network (IPN) of gelatin ionically cross-linked with silicate nanoparticles were engineered by integrating microfabrication with Michael-type addition chemistry and ionic gelation. By encapsulating clinically relevant anchorage-dependent cervical cancer cells and suspension leukemia cells as cell culture models in these composite microgels, we demonstrate enhanced cell spreading, survival, and metabolic activity compared to control gels. The composite bioadhesive hydrogels represent a platform that could be used to study independent effect of stiffness and adhesive ligand density on cell survival and function. We envision that such microarrays of cell adhesive microenvironments, which do not require harsh chemical and UV crosslinking conditions, will provide a more efficacious cell culture platform that can be used to study cell behavior and survival, function as building blocks to fabricate 3D tissue structures, cell delivery systems, and high throughput drug screening devices.

Keywords—Cell adhesive, Microgels, Michael-type addition, Composite hydrogels, Bioadhesive, Cancer, Leukemia.

INTRODUCTION

Cell encapsulated microscale hydrogels and scaffolds have emerged as implantable or injectable biomaterials for the delivery of biological therapeutics,

Address correspondence to Ankur Singh, Sibley School of Mechanical and Aerospace Engineering, Cornell University, Ithaca, NY 14853, USA. Electronic mail: as2833@cornell.edu

This paper is part of the 2014 Young Innovators Issue.

Ankur Singh is an Assistant Professor in the Sibley School of Mechanical & Aerospace Engineering at Cornell University, where he directs the Immunotherapy and Cell Engineering Laboratory. Dr. Singh has expertise in the engineering of biomaterials based platforms for immune cell modulation, cell-biomaterial interactions, cell adhesion, nanoengineered materials, and stem cells. He received his postdoctoral training at Georgia Institute of Technology where he employed engineering and molecular cell biology principles to understand force response and mechanotransduction during the process of human stem cell reprogramming and differentiation. Dr. Singh received his Ph.D. in Biomedical Engineering at The University of Texas at Austin. His research has established multi-modal, synthetic immune priming centers and micro-nanoparticle vaccines for blood cancer and viral infections. His other relevant work includes developing self-assembly nanogels for protein therapeutic delivery to reduce osteoarthritis associated inflammation in knee joints. He has published peer-reviewed paper in Nature Methods, PNAS, Advanced Materials, Molecular Therapy, Biomaterials, Journal of Controlled Release, and Journal of Cell Science. His research is supported by the National Institutes of Health and National Cancer Institute.

Published online: 08 August 2014

and numerous cell-tissue engineering applications. Hydrogel microencapsulation of cells is a promising strategy to support cell growth, modulate its behavior and alongside provide for immunoisolation after transplantation.[16,27,34,38,41] Microarrays of cell-encapsulated hydrogels can be used to study cell behavior and survival, serve as building blocks to fabricate 3D tissues, cell delivery systems, and high throughput drug screening devices.[10] Conventional design considerations for microgels included tunable mechanical and biochemical properties that could support growth of encapsulated cells. A rationally designed scaffold should allow for encapsulated cells to survive, adhere, proliferate, and remodel the niche, as well as deliver growth supporting molecules. Recently the paradigm has shifted towards developing bioengineered hydrogels that recapitulate aspects of the cell-specific microenvironmental conditions in native tissues such as adhesive proteins and architecture.[3–7,9,29,30,35,39] Current 3D tissue or cell culture platforms include multicellular spheroids grown in suspension,[24,28] cells encapsulated within naturally derived ECM such as basement membrane Matrigel,[25,47,48] alginate,[7] collagen,[33] or non-degradable scaffolds fabricated using chemical, thermal or UV cross-linked methods.[2,22]

Polyethylene glycol (PEG) based hydrogels consist of low-protein binding networks with proven minimal immunogenicity that have been widely used for *in vivo* testing.[6,21,35,37,40] A vast majority of PEG-based microgels are prepared using photo, thermal, or emulsion crosslinking approaches using microfluidics.[2,22] In diacrylate functionalized PEG hydrogels, PEG macromers are crosslinked *via* free-radical reaction initiated by chemical activation or UV cleavage of a photoinitiator (e.g., Irgacure®). Such photocrosslinked hydrogels have been extensively studied over the past decade yet a critical drawback of free-radical crosslinking is that it can significantly reduce the viability of encapsulated cells and is unwieldy for *in situ* delivery of cells and biomolecules through surgical needles. Although cell encapsulation in a microfluidic chip generated microgels using emulsification of hydrazide and aldehyde functionalized carbohydrates without free radicals have been reported,[23] bioactive adhesion molecules cannot be easily incorporated in such microgels making the maintenance of cells requiring adhesive ligands for viability and function difficult. Alternatively, hydrogels formed by Michael-type conjugate addition chemistry present a more suitable platform for cell encapsulation, adhesive moiety incorporation, and *in situ* delivery of cells and/or biomolecules.[19,20,32,35,40,42,44] Michael-type addition crosslinking avoids the use of cytotoxic free-radicals and UV light, but instead requires a nucleophilic buffering reagent such as triethanolamine (TEA) or HEPES to facilitate the addition reaction. These hydrogels can be engineered using Michael-type addition reaction by cross-reacting functional groups such as acrylate, vinyl sulfone and maleimide with bi-functional or branched thiolated molecules. We have previously developed *in situ* cross-linkable hydrogels of functionalized PEG and Dextran that can simultaneously deliver multiple biomolecules to modulate cell behavior *in vivo*.[42,44]

Recently, Allazetta *et al.*[2] showed an engineered microfluidic platform to generate Michael-type addition based PEG-vinylsulfone and PEG–thiol microgels with surface tethered biomolecule composition however bulk incorporation of adhesive molecules and cell encapsulation was not examined in these studies. Headen *et al.*[18] reported a microfluidic approach to functionalize 4-arm PEG-maleimide (PEG-MAL) Michael-type addition gels with adhesive peptides. The PEG-MAL hydrogel system has significant advantages over other hydrogel chemistries, such as well-defined hydrogel structure, facile and stoichiometric incorporation of bio-adhesive ligands, increased cellular compatibility, and tunable swelling ratios and reaction rates.[35] Nevertheless, arrays of bio-adhesive PEG-MAL microgels fabricated using Michael-type addition reaction and interpenetrating networks (IPNs) of adhesive proteins have not been reported.

Here we report bioadhesive microgels with modular dimension, mechanical properties and bulk modified adhesive biomolecule composition created by integrating microfabrication with PEG-MAL chemistry and IPNs of gelatin and synthetic silicate nanoparticles in growth media conditions. The resulting system presents an IPN where PEG-MAL is cross-linked with dithiothreitol (DTT) cross-linker *via* Michael-type addition and gelatin is cross-linked to silicate nanoparticles through ionic interactions (Fig. 1a). The composite PEG microgels present cell adhesive motifs for enhanced cell adhesion, spreading, and survival; and are mechanically more stable than gels formed by mixing gelatin with silicate nanoparticles (called gelatin-NP hereafter). These composite PEG hydrogels demonstrate negligible cell-mediated hydrogel size contractions compared to hydrogels formed with gelatin-NP only. By encapsulating clinically relevant anchorage-dependent and suspension cells in these bioadhesive hydrogels, we demonstrate enhanced cell spreading, survival, and metabolic activity compared to control gels. We envision that such cell adhesive microenvironments, which do not require harsh chemical and UV crosslinking conditions, will provide a more efficacious platform for cell and tissue engineering applications and could support controlled cell programming as well as differentiation.

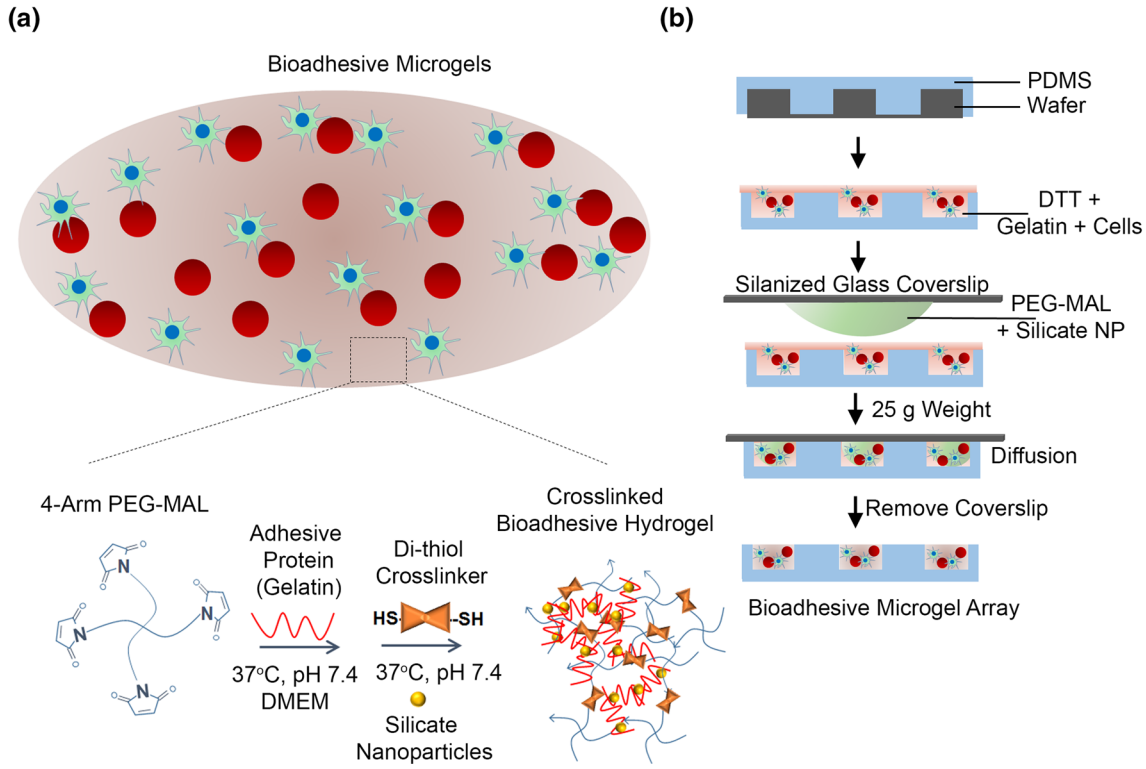

FIGURE 1. Bio-adhesive, cell encapsulated IPN of PEG-MAL and gelatin-silicate nanoparticles (NP). (a) Schematic of bio-adhesive cell supportive microenvironment consisting of 4-arm PEG-MAL crosslinked with DTT and coated with a stable IPN of gelatin with silicate NP. The 4-Arm PEG-MAL undergoes a Michael-type addition reaction with thiol groups on DTT and gelatin forms an ionic gelation complex with NPs at 37 °C and pH 7.4. The PEG component provides structural support for cells while the gelatin-NP component provides adhesive ligands for cell spreading and signaling. Red spheres represent suspension cells and green cells are anchorage-dependent. (b) Schematic representing microfabrication of bio-adhesive microgels. Component A consisting of a well-mixed solution of gelatin with DTT and media with or without cells and poured onto a PDMS microwell mold. Component B consisting of 4-arm PEG-MAL precursors were mixed with silicate NPs and media was placed on a Sigmacote-coated glass slide and aligned with Component A on each micromold, allowing the polymers to diffuse and mix. After 1 min, glass slides were removed leaving behind an array of cell encapsulated microgels.

MATERIALS AND METHODS

Hydrogel Microfabrication

Polydimethylsiloxane (PDMS) microwell molds were fabricated as reported earlier using Sylgard 184 (Dow Corning, MI).[43] The microwells were plasma treated in a Harrick Plasma Cleaner for 2 min to make the microwells hydrophilic. To obtain siliconized glass slides, Sigmacote™ was applied to glass slides, dried, and finally rinsed thoroughly in DI water (Labconco). PEG-MAL (20,000 Da, 99% functionalized) was purchased from Laysan Bio, Inc. and DTT was purchased from Life Technologies. Silicate nanoparticle (Laponite XLG) were obtained from Southern Clay Products, Inc. (Louisville, KY). Type-A porcine skin gelatin was obtained from Sigma Aldrich (Milwaukee, WI).

A 5% w/v mixture of synthetic silicate nanoparticle (NP) in deionized water was prepared and vortexed for 2 min. The mixture transitioned from cloudy to clear, indicating fully exfoliated nanoparticles. A 12.5% w/v mixture of gelatin in DMEM was prepared and heated to 37 °C until the gelatin dissolved. Stock solutions of 0.4% w/v DTT and 25% w/v PEG-MAL in DMEM medium were prepared and kept on ice until ready. It should be noted that gels referred to as 0% PEG essentially means they were composed of gelatin and silicate nanoparticles only. Other composite gels were engineered with 2.5 or 5% PEG-MAL macromer. To fabricate microgels, the precursor solutions were mixed to form two component mixtures (Fig. 1b). Component A consisted of gelatin, DTT, and DMEM. For cell-encapsulated gels, cell suspension was added to component A. Likewise, component B consisted of PEG-MAL, silicate NP, and DMEM. To formulate bulk gels, the two component mixtures were simply mixed at pH 7.4 and heated to 37 °C. To prepare the microgels, a drop of Component A was placed on a plasma treated microwell mold. A small drop of Component B was placed on a siliconized glass slide, which was then aligned on top of the mold and allowed to diffuse through a thin layer of Component A. A 25 g weight was placed on top of the slide to remove

any excess solution. After 1 min the glass slide was removed and the mold with the microgel was placed in media. The siliconization prevented the hydrogel for adhering to the glass slide. Hydrogels were prepared according to the compositions in Table 1 and were cured in growth media conditions for an hour.

Silicate Nanoparticle Cytotoxicity Assay

The effect of silicate NP on the metabolic activity of human cells was determined using MTT assay (ATCC® 30-1010K) according to manufacturer's protocol. In brief, human mesenchymal stem cells were cultured in 96 well plates with density of 2000 cells/cm^2. The pre-seeded cells were subjected to different concentration of nanoparticles (10 μg/mL to 10 mg/mL). After 24 h, media was removed and was replaced with 100 μL of fresh culture medium and 10 μL of MTT solution. 4 h post incubation, lysis buffer was added to each well and was allowed to incubate at 37 °C for 2 h and absorbance was measured at 570 nm.

Hydrolytic Swelling/Degradation and Enzymatic Degradation

50 μL PEG-MAL hydrogels with or without gelatin and silicate NP were prepared in a 500 μL tube. After gelation, hydrogels were weighed and transferred to a 2 mL tubes. Each tube was filled with 200 μL of either PBS (pH 7.4) or 4 mg/mL collagenase IV solution (reconstituted in PBS) for hydrolytic or enzymatic degradation studies, respectively. These hydrogels were incubated at 37 °C on a slow speed rocker. Weight measurements were taken at 0, 8, 12, 24, 48, and 72 h for both hydrolytic and enzymatic degradation sets. Additional weight measurements were taken at 96, 120, 144, and 168 h for the hydrolytic degradation set. After each measurement, fresh PBS or collagenase solution was replenished into each respective tube. Swelling (weight) ratio of these hydrogels was determined using the following relation as reported earlier by us[44]:

$$Q_m = \frac{\text{Weight}(t>0)}{\text{Weight}(t=0)}$$

Dry weight measurements were also performed to determine decrease in polymer mass with hydrogel degradation.[14,17] 50 μL hydrogels were prepared for $t = 0$ and 48 h for both hydrolytic and enzymatic degradation groups. The hydrolytic and enzymatic gels were soaked in PBS and 4 mg/mL collagenase IV solution respectively. All groups at $t = 0$ were immediately dried in an oven at 60 °C and weighed. The $t = 48$ h groups were dried and weighed after possible degradation after 48 h. The degradation was measured as a ratio between the initial dry weight and final dry weight.

Hydrogel Contraction Studies

For matrix contraction studies we used mouse embryonic fibroblast (MEF) cells[8,11] as stromal cell model. MEFs were typsinized, centrifuged, and re-suspended in DMEM at 2×10^8 cells/mL. Cell-laden hydrogels with 5 μL total volume were prepared with 0, 50,000, and 100,000 MEF cells. High cell densities[13] were chosen to maximize contraction in the gels. As previously, component A and component B were combined and allowed to polymerize. Hydrogels were cured for 10 min before DMEM media was added into the well. Images of the whole gel were taken using an EVOS microscope (Life Technologies) at $t = 0$, 24, 48, and 72 h. The area of the 2D projection of the gels were measured using ImageJ.

Rheology

250 μL hydrogels of various compositions were prepared in 500 μL Eppendorf tubes and incubated overnight in PBS at 4 °C. Prior to rheology measurements using the Discovery Hybrid Rheometer from TA Instruments (New Castle, DE), each gel was incubated at 37 °C for 5 min. The storage and loss moduli were measured as a function of frequency that varies from 0.1 to 100 rad/s using 25 mm 2.021° cone-plate geometry.

Cytocompatibility and Spreading of Cancer Cells

TF-1a (ATCC® CRL2451™) leukemia suspension cells and anchorage-dependent cervical cancer HeLa cells were a gift from Prof. Brian Kirby at Cornell University. Cervical cancer HeLa cells were typsinized, centrifuged, and re-suspended at a concentration of 2×10^8 cells/mL in DMEM with 10% FBS and 1% Penicillin/Streptomycin. 20 μL microgels with 400,000 encapsulated cells were prepared according to the procedure above. Separate sets of gels were made for $t = 0$, 24, 48, and 72 h for each studied composition. The gels were stained with Calcein-AM and Ethidium Homodimer-I and imaged using a Nikon TE 2000U florescence microscope. Live and dead cell counts as well as cell spreading measurements were performed using ImageJ. Briefly, both live and dead images were stacked in ImageJ and the stacked images were analyzed for Maxima function that determines the local maxima in a rectangular section of image (i.e., each well) and marks one cell per maximum. This tool counts the number of local maxima of brightness outside a given tolerance, or the number of "bright

TABLE 1. Hydrogel compositions.

Composition	PEG-MAL (w/v %)	DTT (w/v %)	Gelatin (w/v %)	Silicate NP (w/v %)
5PEG+2.5G+1.5NP	5	0.07	2.5	1.5
5PEG+0.5G+0.3NP	5	0.07	0.5	0.3
5PEG+0G+0NP	5	0.07	0	0
2.5PEG+2.5G+1.5NP	2.5	0.03	2.5	1.5
2.5PEG+0.5G+0.3NP	2.5	0.03	0.5	0.3
2.5PEG+0G+0NP	2.5	0.03	0	0
0PEG+2.5G+1.5NP	0	0	2.5	1.5
0PEG+0.5G+0.3NP	0	0	0.5	0.3

These hydrogel compositions were examined in the various experiments performed in this study. They are referred to by the names given in the first column.

spots''. For spreading, the images were preprocessed using a band-pass filter to reduce any noise. Area and circularity ($[\text{circularity}] = 4\pi[\text{area}]/[\text{perimeter}]^2$) measurements were performed using the analyze particles function in ImageJ. Samples were also imaged using confocal microscopy to determine the distribution of the cells.

Co-encapsulation of Adhesive and Suspension Cells

TF-1a leukemia suspension cells and anchorage-dependent cervical cancer HeLa cells were co-encapsulated in microgels using the method described above. Molecular Probes® CellTracker™ fluorescent probes were used to study the co-encapsulation of these cells. TF-1a cells were re-suspended in RPMI media and stained with Cell Tracker™ Orange CMTMR at 37 °C for 30 min. The cells were then centrifuged and re-suspended twice in DMEM to remove excess dye. Adherent HeLa cells were stained with CellTracker™ Green CMFDA at 37 °C for 30 min. A mixture of 1×10^8 TF-1a cells/mL and 5×10^7 HeLa cells/mL in DMEM was prepared. 20 μL micro gels encapsulated with 200,000 TF-1a and 100,000 HeLa cells were prepared according to the procedure above. The gels were imaged on a Nikon TE 2000U florescence microscope at $t = 0$, 24, and 48 h.

Cell Proliferation and Metabolic Activity

For cell proliferation studies, cell numbers and volume was adjusted to fit within the linear range of the metabolic activity assay standard curve over the 6 day study. Three sets of cell combinations were tested: 5,000 HeLa cell, 5,000 TF-1a cells, and 5000 HeLa cells with 5,000 TF-1a cells. A set of microgels for each time point ($t = 0$, 1, 3, and 6 days) was prepared and placed in a 96 wells plate with 100 μL of RPMI medium. For control, bulk and microgels of the studied compositions were prepared without cells. At predetermined time points, CellTiter 96® AQueous One Solution Cell Proliferation assay solution (Promega, 20 μL reagent/100 μL medium) was added to each well and incubated for 4 h at 37 °C and 5% CO_2. The fluid was transferred to a new well plate and centrifuged. Supernatant was analyzed using a BioTek plate reader at 490 nm. Proliferation was evaluated using the fold increase in the measured absorbance.

Statistics

Analysis of variance (ANOVA) statistical analyses were performed using GraphPad Prism 9.1 software with Tukey's test for pairwise comparisons. For cell spreading analysis across Different time points, ANOVA was performed with Bonferroni correction. For studies involving effect of hydrogel mechanical properties on cell survival, ANOVA was performed with Tukey's correction. A p value of less than 0.05 was considered significant. All studies were performed in triplicates unless otherwise noted. All values are reported as mean ± SE.

RESULTS AND DISCUSSION

Approaches to fabricate cell encapsulated PEG-based microgels using Michael-type addition reaction have been few[2,18] and arrays of bioadhesive PEG-MAL microgels with IPNs of adhesive proteins demonstrating cell encapsulation have not been reported. We have developed an array of bioadhesive PEG-MAL microgels using a simple microwell approach (Fig. 1b). These microgels present a cell supportive microenvironment with adhesivity and tunable swelling, mechanical, and degradation properties. We identified that addition of silicate NP in gelatin solution at 37 °C results in formation of a hydrogel that prevents liquefaction of gelatin at 37 °C (Fig. 2a). Polyampholytic gelatin, containing positively and negatively charged regions, strongly interacts with the anisotropically distributed opposite charges on the synthetic silicate NPs (20–30 nm in diameter and ~1 nm in thickness), as an outcome of which gelatin remains stable and does not liquefy at 37 °C.

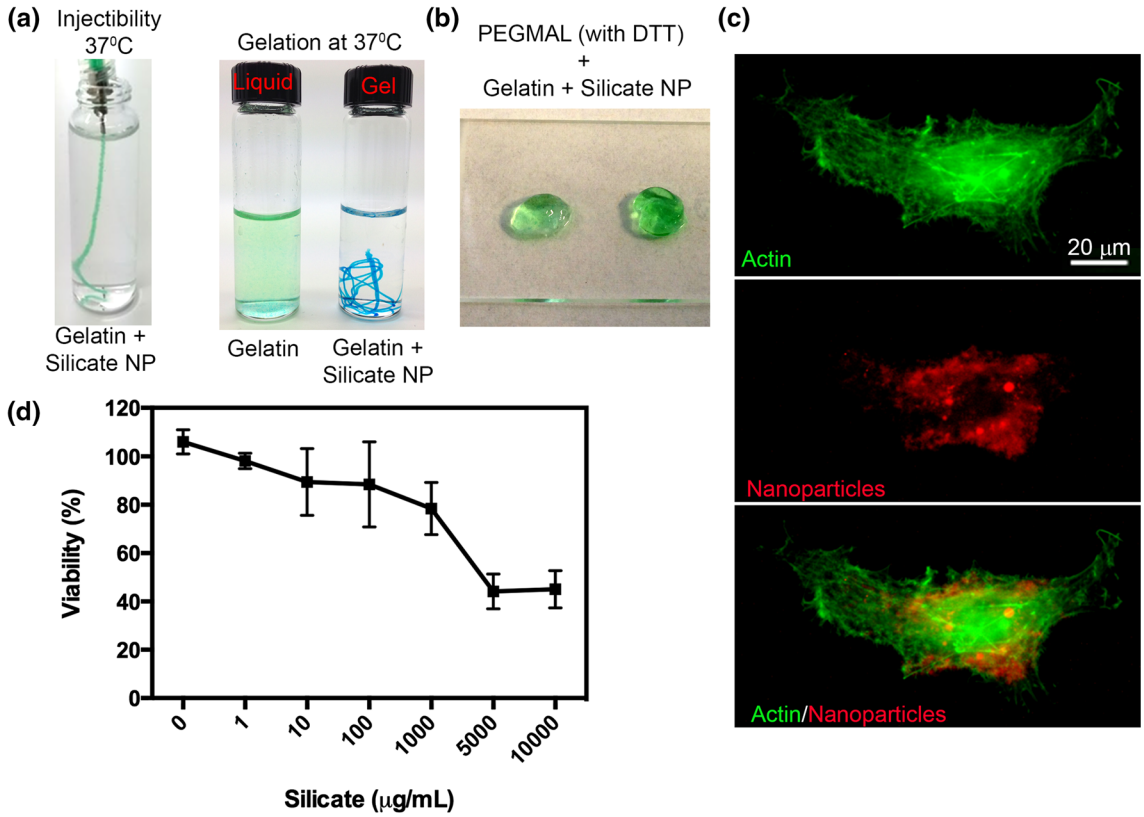

FIGURE 2. Gelatin crosslinking with silicate nanoparticles. (a) Image indicates the injectability and stability of gelatin at 37 °C in presence of NP while gelatin alone liquefies. (b) Image indicates representative bulk gels formed with DTT crosslinked PEG-MAL with incorporated gelatin-silicate NPs. (c) Confocal images of cellular uptake of silicate NP. (d) Cell metabolic activity at increasing dose of silicate NPs.

The gelatin-NP hydrogel was used as an adhesive IPN with a PEG-MAL network cross-linked with DTT (Fig. 2b), which otherwise is non-adhesive in nature. In these studies, composite hydrogels of PEG-MAL and gelatin-NP were called IPNs.[45] Gelatin silicate hydrogels without any PEG-MAL component or vice versa were not considered IPNs. The rationale for using DTT was that the di-thiols provide an easy and fast reacting cross-linker that is non-degradable and prevents any cell spreading if no other degradable matrix is present.[26] Previous studies have demonstrated that DTT incorporated hydrogels with DTT concentrations up to 70 mM do not cause significant cytotoxicity.[36] In our studies we used DTT at a maximum concentration of 4.5 mM. Another potential concern was the cytotoxicity of silicate NPs. As indicated in Fig. 2c, the freely available nanoparticles were readily taken up by the human cells, indicating the cytocompatible behavior and maintained >80% cell viability up to 1000 μg/mL concentration (Fig. 2d). In our studies, the concentration of nanoparticles was below this threshold limit. Our results are in good correlation with previously reported findings by Gaharwar *et al.*[15] that silicate nanoparticles are cytocompatible.

We explored the effect of network composition, presence and absence of gelatin-NPs within PEG-MAL networks on hydrolytic swelling and degradation. We compared bulk gel compositions consisting of 5% PEG-MAL and 2.5% PEG-MAL with varying weight percentages of gelatin-NP (Figs. 3a and 3b). As expected for hydrogels containing no gelatin-NP, 5% PEG-MAL hydrogels swelled significantly more than 2.5% PEG-MAL gels ($p < 0.05$), with swelling ratio (Qm) 3.17 and 1.5, respectively. This difference in swelling can be attributed to higher proportions of hydrophilic PEG in 5% gels compared to 2.5% PEG-MAL gels. Similarly, 2.5% PEG-MAL with gelatin-NP swelled significantly less than their 5% counterpart ($p < 0.05$), irrespective of gelatin-NP percentages. Within the same w/v % of PEG-MAL, no significant difference in swelling ratio was observed with incorporation of gelatin-NP. Hydrogels containing only gelatin-NP showed significantly higher degradation than PEG containing gels, losing approximately half their weight within 48 h. These experiments were continued for 7 days with no significant change in normalized weight ratios compared to 48 h time point.

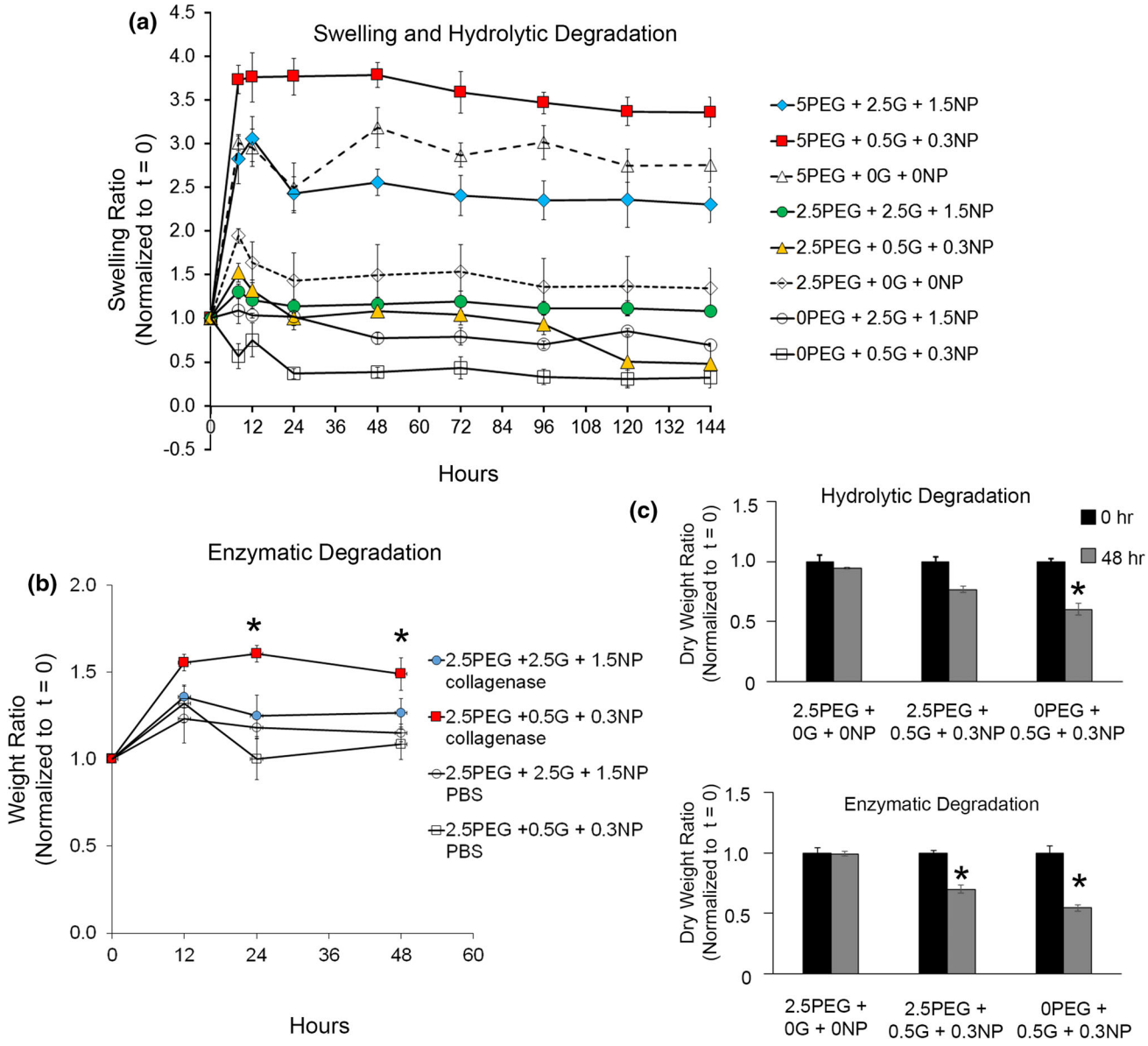

FIGURE 3. Hydrogel swelling and degradation. (a) Swelling and degradation profiles of various crosslinking network formulations under hydrolytic conditions, (b) network degradation profile when enzymatically treated with collagenase. (*$p < 0.05$ with respect to gels not exposed to collagenase, $n = 3$). (c) Ratio between dry weight at 0 and 48 h for various compositions under hydrolytic and enzymatic conditions ($n = 3$).

Previous studies have demonstrated that matrix metalloproteinase-mediated degradability of 3D cell culture is desirable because it allows for matrix remodeling, cell spreading, and migration within PEG-based networks.[1,37] Since gelatin is prone to degradation in presence of proteases like collagenase secreted by cells, we assessed change in weight in bulk gels made of 2.5% PEG-MAL with varying weight % of gelatin-NP in presence and absence of enzyme. As indicated in Fig. 3b, with 2.5% PEG-MAL hydrogels modified with 0.5% gelatin and 0.3% NPs, we observed approximately two-fold increase in hydrogel weight when exposed to collagenase for 24 h compared to the gels not treated with collagenase ($p < 0.05$). With 2.5% PEG-MAL hydrogels containing 2.5% gelatin and 1.5% NPs, the increase in weight ratio was only 1.2-fold ($p > 0.05$) compared to untreated counterparts, which could be attributed to the presence of more number of silicate NPs preventing degradation and swelling. We anticipated this behavior because with degrading gelatin network, the cross-linked architecture would change causing an increase in absorption of aqueous media.

To determine decrease in polymer mass because of degradation, we performed dry weight measurements on the hydrogels over 48 h exposure to PBS or

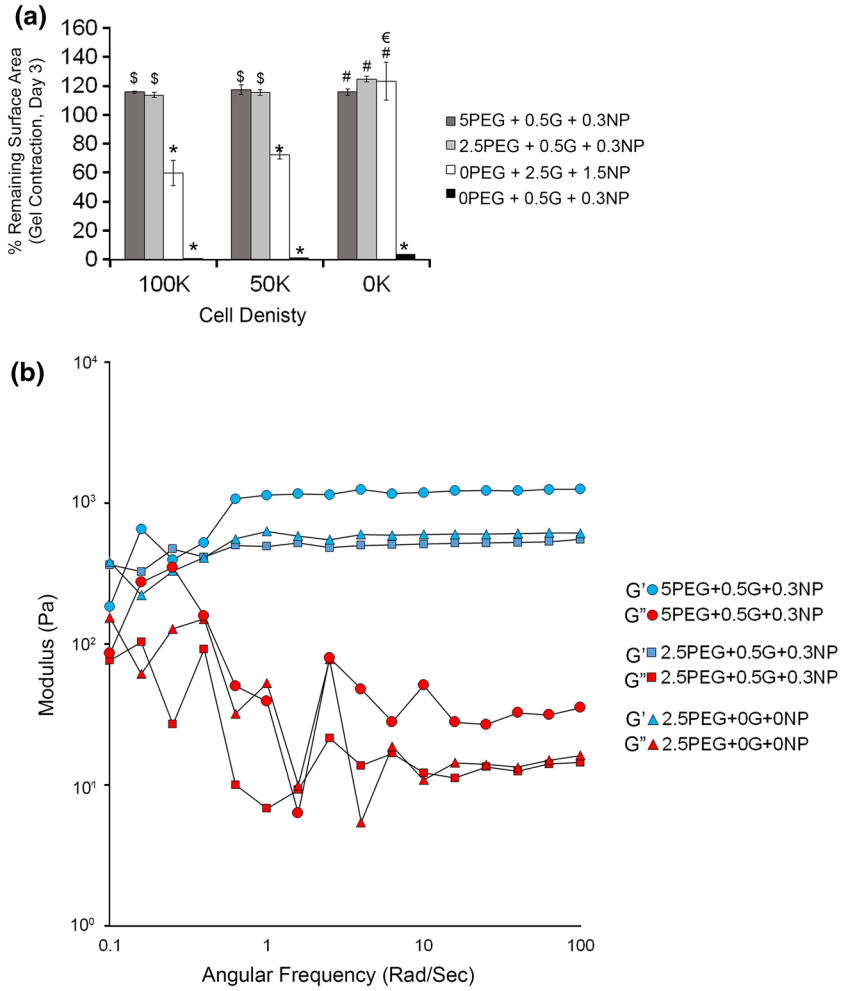

FIGURE 4. Mechanical properties of composite hydrogels. (a) Cell-mediated contraction of hydrogels. The gels were formed, on a 24 well tissue culture plate, from varying proportions of the stock solutions and indicated number of cells. Bar graph represents the percent of hydrogel bottom surface area remaining at day 3 (compared to day 0). *$p < 0.05$ compared to all other groups at a particular cell density; $^{\$}p < 0.05$ compared to gelatin-NP only gels at a particular cell density; $^{\#}p < 0.05$ compared to 0.5G+0.3NP gels at a particular cell density; $^{€}p < 0.05$ for a group across different seeding density; $n = 3$. (b) The viscoelastic behavior of the PEG-MAL and PEG-MAL composite IPNs was studied by measuring the *G′* and *G″* moduli of the gels as a function of frequency.

collagenase (Fig. 3c). With PBS, no significant change in dry mass was observed for PEG only gels and 2.5% PEG-MAL hydrogels containing 0.5% gelatin and 0.3% NPs. For hydrogels consisting only of gelatin-NPs and no PEG component (called 0% PEG), a significant decrease to 52% dry weight was observed over 48 h ($p < 0.05$). This observation supports our hypothesis that the composite bioadhesive hydrogels of PEG-MAL with gelatin-NPs are more mechanically stable than the ones without PEG, under hydrolytic conditions.

With collagenase, a significant 30% decrease in dry weight was observed for PEG-MAL hydrogels with gelatin-NPs which could be attributed to the degradation of gelatin component. In absence of PEG, gelatin-NP gels showed significant 50% degradation in collagenase ($p < 0.05$) compared to PEG only gels but was not significantly different than PEG-gelatin-NP composite gels. It should however be noted that all 0.5% gelatin with 0.3% NP hydrogel were unstable in absence of PEG and disintegrated into pieces demonstrating mechanical instability of these gels.

Previous studies by Swartz and colleagues have shown that culture of spread fibroblastic cells in a 3D collagen-only matrices (2.5 mg/mL type I collagen) contracted the matrix to 20% of its original size within 72 h making long-term culture difficult.[46] Since our goal is to establish a 3D-cell culture platform for long term studies, we anticipated the gelatin-NP gels to contract upon cell encapsulation. Based on swelling studies, we expected the hydrogels to swell and the presence of cells to counteract such swelling. As indicated in Fig. 4a, 5% PEG-MAL with 0.5% gelatin and 0.3% NP and 2.5% PEG-MAL with 0.5% gelatin and

0.3% NP showed no significant gel contraction ($p > 0.05$) for all cell counts compared to hydrogels with no cells. On the other hand, 2.5% gelatin and 1.5% NP with no PEG showed significant contraction at 50,000 and 100,000 cell seeding density ($p < 0.05$). As discussed earlier, the 0.5% gelatin and 0.3% NP disintegrated into small pieces for all cell counts by day 3 independent of the cell count indicating mechanical instability of the bulk gels. These studies demonstrate that by incorporating minimal amount of gelatin-NPs, we can control the swelling ratio, degradation kinetics, as well as cell induced contraction of matrices.

We next examined the effect of gelatin-NP incorporation on stiffness of bulk PEG-MAL hydrogels. All rheological measurements were performed on swollen hydrogels equilibrated in PBS and the storage and loss moduli were plotted as a function of angular frequency (Fig. 4b). Rheological characterization of the adhesive and non-adhesive hydrogels was performed with similar PEG concentration to examine the effect of gelatin-NP incorporation on hydrogel stiffness. There was no difference in the storage modulus with incorporation of gelatin-NPs indicating that incorporation of adhesive components in the bulk PEG-MAL hydrogel does not affect its viscoelastic properties. Furthermore, the storage moduli of 5% PEG hydrogels were higher than the 2.5% PEG hydrogels for the same amount of adhesive ligands, indicating increased stiffness with increasing polymer concentration, independent of adhesive ligand incorporation.

The main aspect of this study was to transform the PEG-MAL-based adhesive gels into microgels. We next manufactured micron-scale hydrogels using a simple microwell technique. Microgels were prepared in a two-step process where Component A consisting of gelatin, DTT, and DMEM media (with cells if applicable) was poured onto the microfabricated PDMS wells (Fig. 1b). Typically 3–4 microwell constructs each carrying 500 wells were placed on a glass slide and Component B (PEG-MAL, silicate nanoparticle, and DMEM media) was slowly placed on top of each construct with Component A. After 1 min the glass slide was gently removed and the mold with the microgels was submerged under growth media. All gels formed in <5 min, even at the lowest concentration of PEG-MAL and gelatin-NPs. We did not observe overlapping regions of polymer gel network between individual wells, except occasionally with gelatin-NP formulations only (particularly at higher w/v % of gelatin and NP).

To demonstrate the PEG-MAL (DTT) with gelatin-NPs as a cytocompatible interpenetrating microenvironment for cell encapsulation, cervical cancer HeLa cells were encapsulated in ECM mimetic hydrogels using the 5 or 2.5 w/v % PEG-MAL formulation with 0.5% gelatin and 0.3% NP or 2.5% gelatin with 1.5% NP. Following polymerization, the cervical cancer cell laden microgels were cultured under standard growth conditions, and cell viability was assessed at 24, 48 and 72 h using Live/Dead staining, which discriminates dead cells (red) from viable cells (green) based on membrane integrity (Figs. 5a). We analyzed 16 wells per sample to determine percentage of live cells. Quantitative analysis of images obtained from fluorescence microscopy indicated excellent cell viability $84 \pm 1.7\%$ after 24 h in microgels formed with IPNs of 5% PEG-MAL with 0.5% gelatin and 0.3% NPs, which however was significantly reduced to $75 \pm 1.7\%$ after 72 h (Fig. 5b). On the other hand, bioadhesive microgels of 2.5% PEG-MAL with 0.5% gelatin and 0.3% NP composition indicated excellent $87 \pm 0.09\%$ viability over 24 h and increased to $92 \pm 0.7\%$ over 72 h. 5 and 2.5% PEG-MAL microgels with no gelatin and NPs demonstrated 89 ± 1.1 and $87 \pm 1.3\%$ viable cervical cancer cells respectively. After 72 h, these control PEG-MAL microgels without gelatin-NPs demonstrated only $62 \pm 1.2\%$ viability with 5% PEG-MAL, and $78 \pm 1.4\%$ with 2.5% PEG-MAL gels. Finally, microgels containing only 0.5% gelatin with 0.3% NP showed nearly 80% viability over 72 h. These differences in cell viability with PEG-based gels could be explained based on the differences observed in mechanical properties, degradability (allowing matrix remodeling), and cell spreading behavior as discussed in later sections. Confocal imaging further confirmed that the cells remain well distributed inside the hydrogel over 72 h (Fig. 5c).

Interestingly, when cultured in 2.5% PEG-MAL microgels with same mechanical strength (based on bulk gel analysis), cell survival significantly increased with incorporation of adhesive ligand (Fig. 6). When the ligand density was kept same (0.5% gelatin with 0.3% NP), increase in hydrogel stiffness from 550 to 1100 Pa with increasing PEG% resulted in significant reduction in cell survival. The enhanced survival in 2.5% PEG gels with adhesive ligands could be attributed to integrin mediated cell adhesion and lower crosslinking density of the polymer compared to 5% PEG gels. These finding are further supported by our observations that 5% PEG-MAL gels with no adhesive ligand showed significantly lower cell survival than 5% PEG-MAL with adhesive components. Therefore, these composite microgels could be used to study independent effect of stiffness and ligand density on cell survival and functioning.

We next evaluated the effect of bioadhesive microgels on cell spreading by measuring the average cell area and average circularity of micro-encapsulated HeLa cells (Fig. 7a). As mentioned earlier, one of the rationale for using DTT as a cross-linker was to

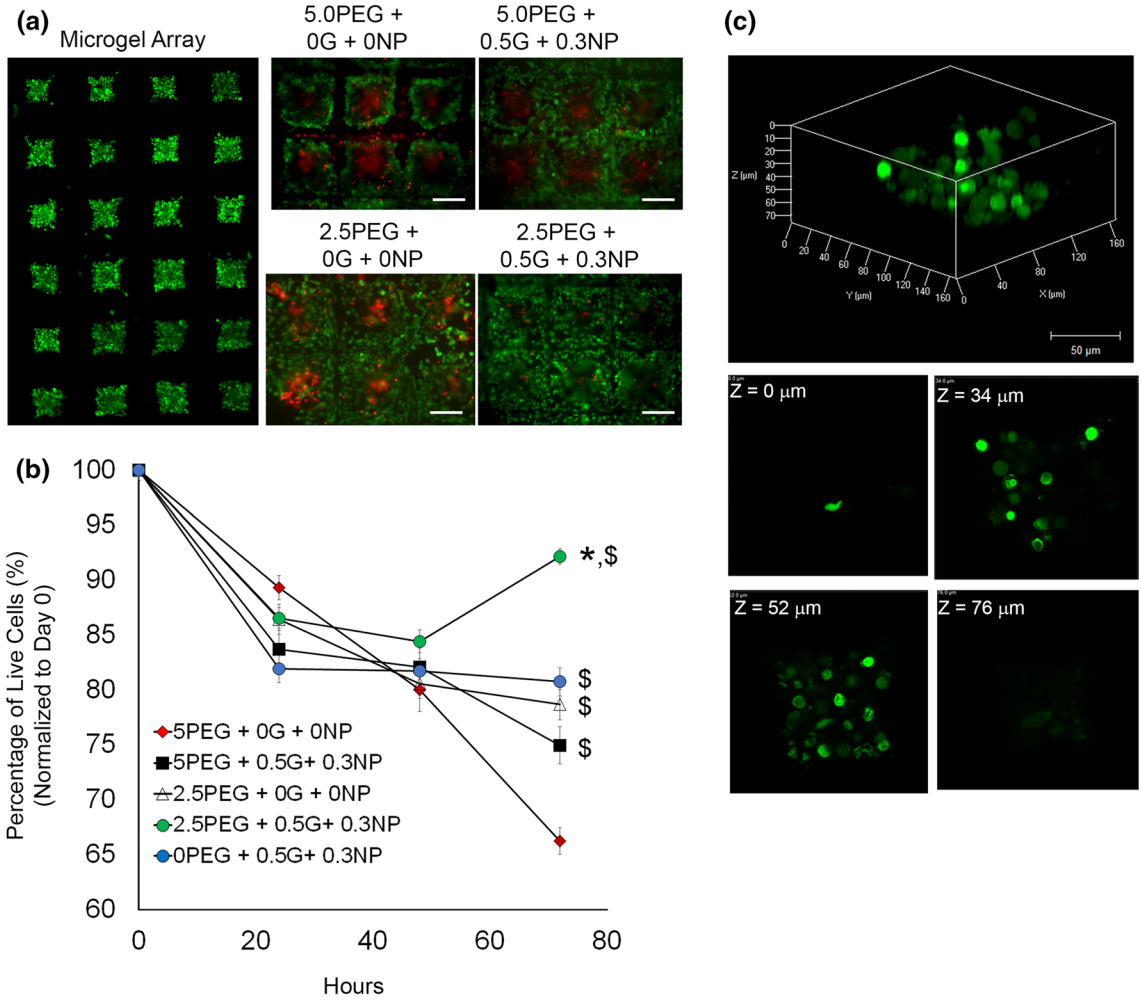

FIGURE 5. Live/Dead cytotoxicity studies. (a) Fluorescent micrograph of a representative microgel array at $t = 0$. Individual panels for each microgel group represents live (green) and dead (red) cells on day 3. Scale Bar = 200 μm. (b) Scatter plot of cell viability profiles for each microgel formulation over a period of 72 h. All samples were seeded with 4×10^5 cells at $t = 0$. Data represents % survival normalized to $t = 0$. *$p < 0.05$ compared to all other groups at 72 h; $^{\$}p < 0.05$ compared to 5% PEG-MAL only gels (red) at 72 h. $n = 16$. (c) 3D reconstruction of a whole 2.5P+0.5G+0.3NP microgel with individual z-sections at indicated depth.

prevent any matrix-degradation mediated spreading of cells. At $t = 0$, the encapsulated cells were spherical in shape. At $t = 48$ h, we did not observe any spreading in PEG-MAL microgel ($p > 0.05$) and marginal spreading in 0.5% gelatin with 0.3% NPs microgels (no PEG-MAL, $p > 0.05$) compared to their respective day 0 average cell spreading areas (Fig. 7b). Notably, it was only the microgels formed with 2.5% PEG-MAL with 0.5% gelatin and 0.3% NP that showed significant spreading ($p < 0.05$) compared to day 0 cells in the same microgels and compared to all other groups at day 2. Importantly, when compared across all formulation, microgels made of 2.5% PEG-MAL with 0.5% gelatin and 0.3% NP clearly demonstrated a superior microenvironment that supported cell spreading and survival. Cell spreading is supported by favorable mechanical properties, bioadhesivity, and enzymatic degradability of gelatin components allowing niche remodeling. Our observations are further supported by previous studies by Fairbanks *et al.*,[12] where spreading of anchorage-dependent cells in lower crosslinking density PEG hydrogels was significantly affected by the concentration of adhesive moiety RGD and gel degradability. We further evaluated the circularity of these cells with lower circularity indicative of cell spreading. As indicated in Fig. 7c, microgels made of 2.5% PEG-MAL with 0.5% gelatin with 0.3% NP demonstrated significantly lower ($p < 0.05$) average cell circularity values further confirming that this particular compositions supports cell spreading. These results clearly demonstrate the significant effect of gelatin incorporation and hydrogel remodeling on HeLa cell spreading and survival. This spreading behavior is not unique to HeLa cancer cells and we observed similar spreading behavior with encapsulated mouse embryonic fibroblasts suggesting the cell supportive

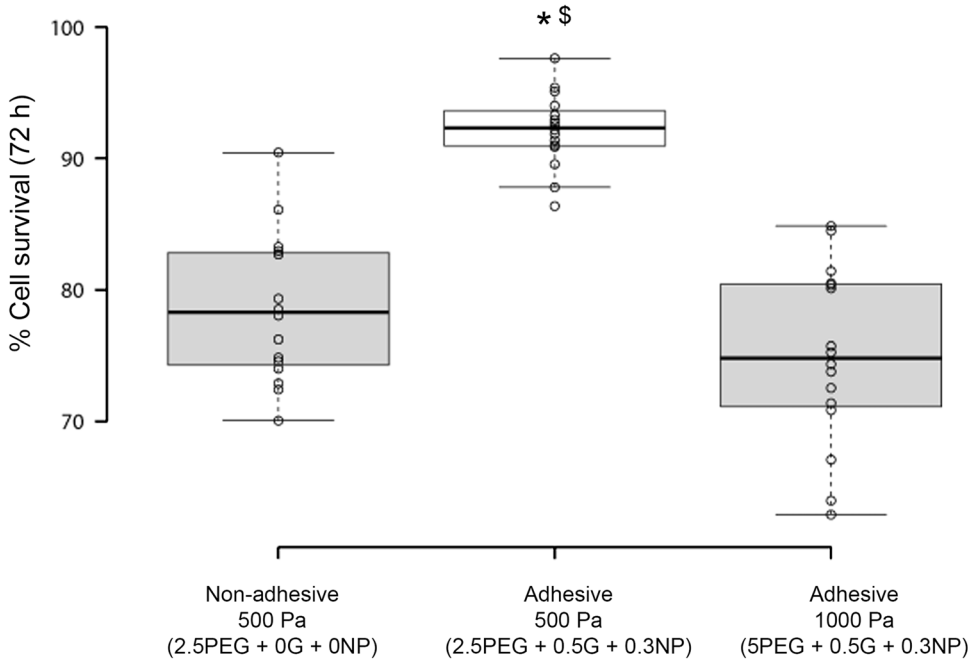

FIGURE 6. Effect of hydrogel stiffness on cell survival. Box plot represents percent cell survival of HeLa cells after 72 h of culture in microgels with approximately 550 and 1100 Pa storage modulus, as determined from bulk gels analysis at 10 kHz frequency. $n = 16$. $^{*}p < 0.05$ compared to non-adhesive hydrogels with same 500 Pa modulus; $^{\$}p < 0.05$ compared to adhesive hydrogels with 1000 Pa modulus. All adhesive hydrogels were composed of equivalent amount of adhesive ligand.

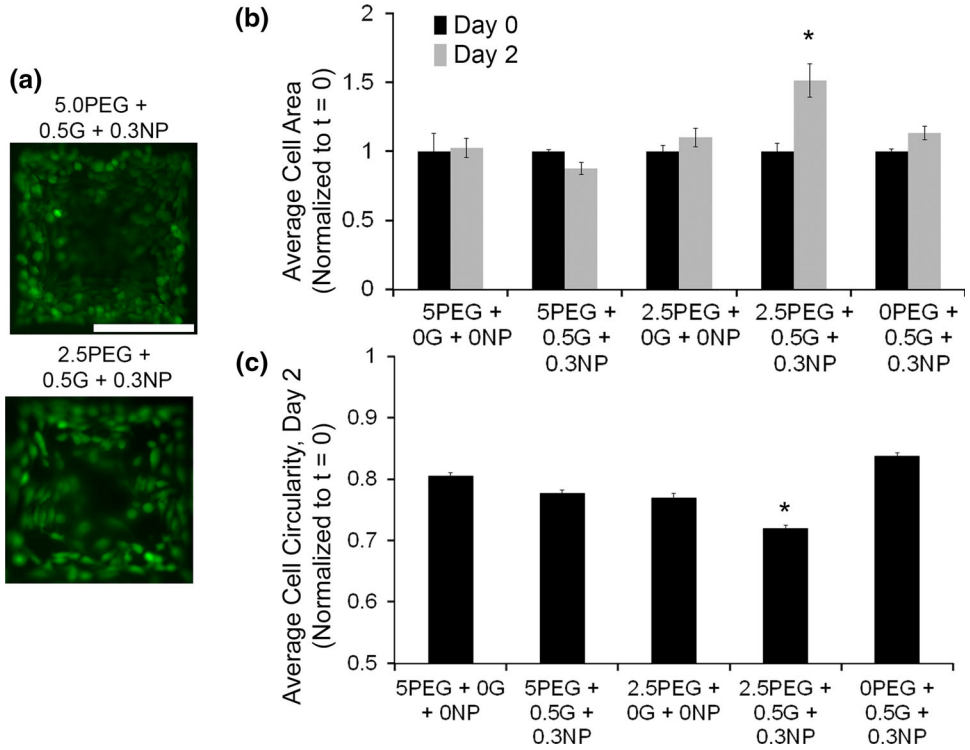

FIGURE 7. Anchorage-dependent cell spreading. (a) Fluorescence micrographs represent spreading behavior of encapsulated HeLa cells in representative microgel formulations. (b) Bar graph represents average cell spreading for each microgel group, normalized to day 0 spreading areas. $^{*}p < 0.05$ compared to all microgel groups on day 2. $n = 5$. (c) Bar graph represents average cell circularity indicative of change in cells shape and spreading. $^{*}p < 0.05$ between compared all other microgel groups. $n = 6$.

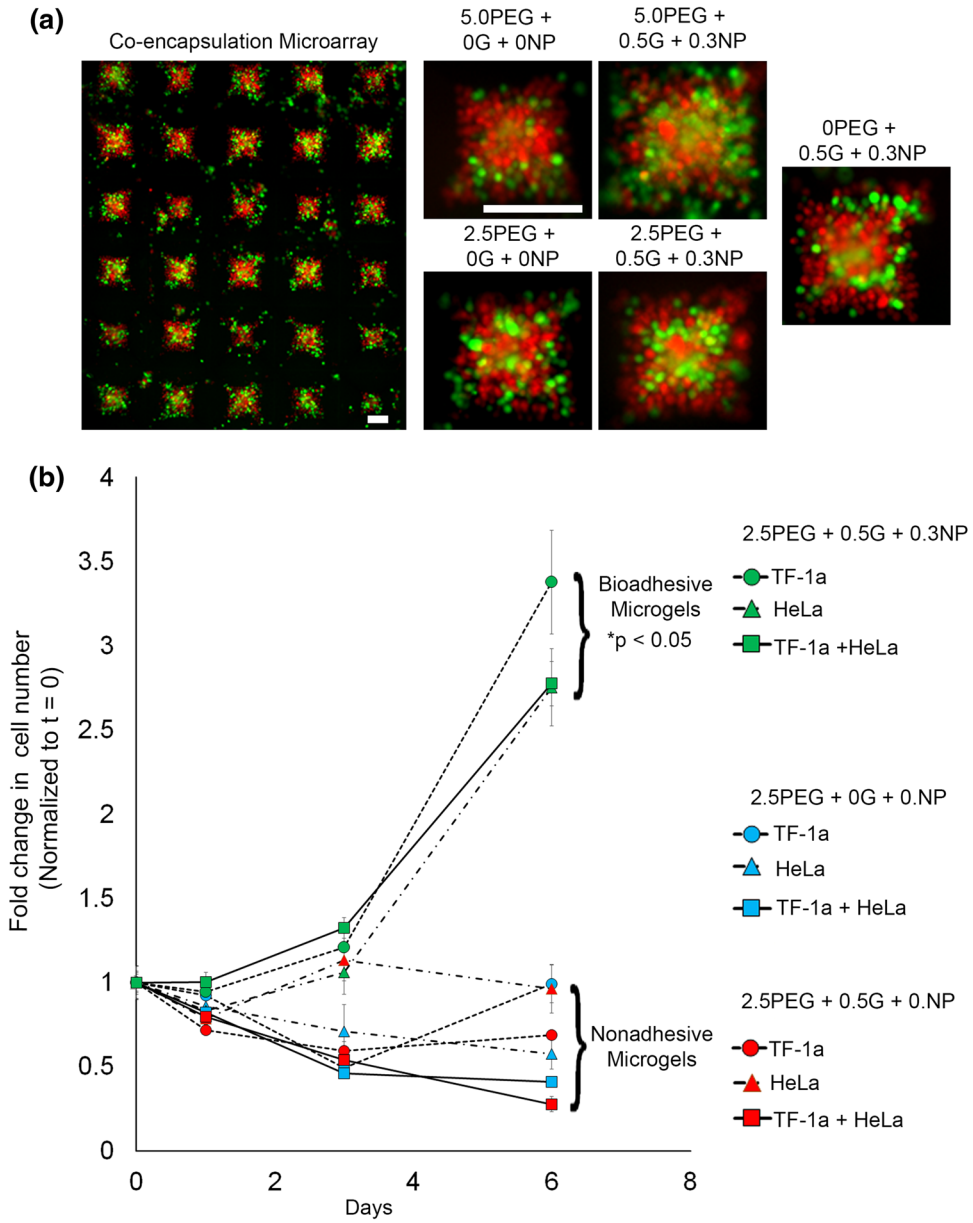

FIGURE 8. Suspension cell co-encapsulation and long term metabolic activity. (a) A suspension of 2 × 10^5 TF-1a leukemia and 1 × 10^5 adhesive HeLa cells, pre-stained with Cell Tracker™ Orange and Cell Tracker™ Green, respectively, were co-encapsulated inside each microgel. Scale Bar = 200 μm. (b) *In vitro* cell proliferation (metabolic activity) was assessed in microgels using CellTiter 96® AQueous One Solution Cell Proliferation assay solution. *$p < 0.05$ compared to nonadhesive microgel groups. $n = 3$.

microenvironment could support other anchorage-dependent cell types.

The final aspect of this study was to explore the potential of PEG-MAL hydrogels with gelatin-NPs for co-encapsulation of suspension and anchorage dependent cells. Such co-culture supportive microenvironments are relevant for bone-marrow and lymphoid tissues. For proof of concept, we co-encapsulated TF-1a leukemia suspension cells and anchorage-dependent HeLa cervical cancer cells that could possibly mimic the rare occurrence of cervical cancer in patients with leukemia.[31] Co-encapsulation results (Fig. 8a) clearly indicate successful encapsulation of both cell types with uniform distribution. These cells were viable over 48 h and in some samples we observed HeLa cell spreading at day 2, however further investigation is required to establish the effect of co-encapsulation on cell adhesivity and integrin-mediated signaling. Similar to our previous observations, 2.5% PEG-MAL with gelatin-NP outperformed other groups. We finally assessed whether the encapsulated cells in co-culture were metabolically active and proliferative compared to individual cell cultures. As indicated in Fig. 8b, all three cell cultures demonstrated significantly ($p < 0.05$)

higher proliferation rate over a week in bioadhesive microgels as compared to non-adhesive PEG-MAL only gels (cross-linked with DTT) or PEG-MAL with gelatin but no silicate NP (allowing liquefaction of gelatin at 37 °C). Taken together, these studies demonstrate the feasibility to co-encapsulate suspension and anchorage-dependent cells together in a growth supportive microenvironment where the both cell types remain metabolically active.

CONCLUSION AND FUTURE DIRECTIONS

In summary, this study presents a facile approach to micro-manufacture arrays of bio-adhesive PEG-MAL microgels using Michael-type addition reaction and IPNs of adhesive protein, gelatin, such that gelatin remains stable and provides a cell supportive microenvironment under normal cell culture conditions. The ease of fabrication, cytocompatible reaction conditions, tunable swelling, enzymatic degradation, and mechanical properties render this microgel platform useful for a wide range of cell and tissue engineering applications. Future investigation will focus on evaluating the ability of these gels to promote primary cell survival and growth as well as for therapeutic delivery of bioactive molecules. Use of 4-arm PEG-MAL could further allows for conjugate addition of thiolated growth factors to one of the PEG arms to engineer cell-instructive matrices for controlled cell programming as well as differentiation. Silicate nanoparticles have been shown to preferentially induce osteogenic differentiation of human mesenchymal stem cells, therefore, we anticipate that such matrices could also provide suitable 3D niches for stem cell differentiation.

ACKNOWLEDGMENTS

The authors would like to acknowledge financial support by Grants from the National Institutes of Health (1R21CA185236-01) and the Cornell University-Ithaca and Weill Cornell Medical College seed grant. The authors also thank Prof. Marjolein C.H. van der Meulen in the Department of Biomedical Engineering and the Sibley School of Mechanical and Aerospace Engineering for providing cells. The authors also thank Dr. Brian Kirby in Sibley School of Mechanical and Aerospace Engineering at Cornell University for access to the cells, microscopy facility and spectrophotometer. The content is solely the responsibility of the authors and does not necessarily represent the official views of the National Cancer Institute or the National Institutes of Health.

CONFLICT OF INTEREST

Ravi Ghanshyam Patel, Alberto Purwada, Leandro Cerchietti, Giorgio Inghirami, Ari Melnick, Akhilesh Gaharwar, and Ankur Singh declare that they have no conflicts of interest.

ETHICAL STANDARDS

No animal or human studies were carried out by the authors for this article.

REFERENCES

[1]Alge, D. L., M. A. Azagarsamy, D. F. Donohue, and K. S. Anseth. Synthetically tractable click hydrogels for three-dimensional cell culture formed using tetrazine-norbornene chemistry. *Biomacromolecules* 14(4):949–953, 2013.

[2]Allazetta, S., T. C. Hausherr, and M. P. Lutolf. Microfluidic synthesis of cell-type-specific artificial extracellular matrix hydrogels. *Biomacromolecules* 14(4):1122–1131, 2013.

[3]Anseth, K. S., A. T. Metters, S. J. Bryant, P. J. Martens, J. H. Elisseeff, and C. N. Bowman. *In situ* forming degradable networks and their application in tissue engineering and drug delivery. *J. Control Release* 78(1–3):199–209, 2002.

[4]Benton, J. A., C. A. DeForest, V. Vivekanandan, and K. S. Anseth. Photocrosslinking of gelatin macromers to synthesize porous hydrogels that promote valvular interstitial cell function. *Tissue Eng. Part A* 15(11):3221–3230, 2009.

[5]Benton, J. A., B. D. Fairbanks, and K. S. Anseth. Characterization of valvular interstitial cell function in three dimensional matrix metalloproteinase degradable PEG hydrogels. *Biomaterials* 30(34):6593–6603, 2009.

[6]Burdick, J. A., and K. S. Anseth. Photoencapsulation of osteoblasts in injectable RGD-modified PEG hydrogels for bone tissue engineering. *Biomaterials* 23(22):4315–4323, 2002.

[7]Chaudhuri, O., S. T. Koshy, C. Branco da Cunha, J. W. Shin, C. S. Verbeke, K. H. Allison, and D. J. Mooney. Extracellular matrix stiffness and composition jointly regulate the induction of malignant phenotypes in mammary epithelium. *Nat. Mater.* 2014. doi:10.1038/nmat4009.

[8]Coyer, S. R., A. Singh, D. W. Dumbauld, D. A. Calderwood, S. W. Craig, E. Delamarche, and A. J. Garcia. Nanopatterning reveals an ECM area threshold for focal adhesion assembly and force transmission that is regulated by integrin activation and cytoskeleton tension. *J. Cell Sci.* 125(21):5110–5123, 2012.

[9]DeForest, C. A., B. D. Polizzotti, and K. S. Anseth. Sequential click reactions for synthesizing and patterning three-dimensional cell microenvironments. *Nat. Mater.* 8(8):659–664, 2009.

[10]Dolatshahi-Pirouz, A., M. Nikkhah, A. K. Gaharwar, B. Hashmi, E. Guermani, H. Aliabadi, G. Camci-Unal, T. Ferrante, M. Foss, D. E. Ingber, and A. Khademhosseini. A combinatorial cell-laden gel microarray for inducing osteogenic differentiation of human mesenchymal stem cells. *Sci. Rep.* 4:3896, 2014.

[11]Dumbauld, D. W., T. T. Lee, A. Singh, J. Scrimgeour, C. A. Gersbach, E. A. Zamir, J. P. Fu, C. S. Chen, J. E. Curtis, S. W. Craig, and A. J. Garcia. How vinculin regulates force transmission. *Proc. Natl. Acad. Sci. USA* 110(24):9788–9793, 2013.

[12]Fairbanks, B. D., M. P. Schwartz, A. E. Halevi, C. R. Nuttelman, C. N. Bowman, and K. S. Anseth. A versatile synthetic extracellular matrix mimic via thiol-norbornene photopolymerization. *Adv. Mater.* 21(48):5005–5010, 2009.

[13]Frampton, J. P., M. R. Hynd, M. L. Shuler, and W. Shain. Fabrication and optimization of alginate hydrogel constructs for use in 3D neural cell culture. *Biomed. Mater.* 6(1):015002, 2011.

[14]Gaharwar, A. K., V. Kishore, C. Rivera, W. Bullock, C. J. Wu, O. Akkus, and G. Schmidt. Physically crosslinked nanocomposites from silicate-crosslinked PEO: mechanical properties and osteogenic differentiation of human mesenchymal stem cells. *Macromol. Biosci.* 12(6):779–793, 2012.

[15]Gaharwar, A. K., S. M. Mihaila, A. Swami, A. Patel, S. Sant, R. L. Reis, A. P. Marques, M. E. Gomes, and A. Khademhosseini. Bioactive silicate nanoplatelets for osteogenic differentiation of human mesenchymal stem cells. *Adv. Mater.* 25(24):3329–3336, 2013.

[16]Gaharwar, A. K., N. A. Peppas, and A. Khademhosseini. Nanocomposite hydrogels for biomedical applications. *Biotechnol. Bioeng.* 111(3):441–453, 2014.

[17]Gaharwar, A. K., C. Rivera, C. J. Wu, B. K. Chan, and G. Schmidt. Photocrosslinked nanocomposite hydrogels from PEG and silica nanospheres: structural, mechanical and cell adhesion characteristics. *Mater. Sci. Eng. C* 33(3):1800–1807, 2013.

[18]Headen, D. M., G. Aubry, H. Lu, and A. J. García. Microfluidic-based generation of size-controlled, biofunctionalized synthetic polymer microgels for cell encapsulation. *Adv. Mater.* 26(9):3003–3008, 2014.

[19]Hiemstra, C., L. J. Aa, Z. Zhong, P. J. Dijkstra, and J. Feijen. Rapidly *in situ*-forming degradable hydrogels from dextran thiols through Michael addition. *Biomacromolecules* 8(5):1548–1556, 2007.

[20]Hiemstra, C., L. J. van der Aa, Z. Zhong, P. J. Dijkstra, and J. Feijen. Novel *in situ* forming, degradable dextran hydrogels by Michael addition chemistry: synthesis, rheology, and degradation. *Macromolecules* 40(4):1165–1173, 2007.

[21]Huebsch, N., P. R. Arany, A. S. Mao, D. Shvartsman, O. A. Ali, S. A. Bencherif, J. Rivera-Feliciano, and D. J. Mooney. Harnessing traction-mediated manipulation of the cell/matrix interface to control stem-cell fate. *Nat. Mater.* 9(6):518–526, 2010.

[22]Hutson, C. B., J. W. Nichol, H. Aubin, H. Bae, S. Yamanlar, S. Al-Haque, S. T. Koshy, and A. Khademhosseini. Synthesis and characterization of tunable poly(ethylene glycol): gelatin methacrylate composite hydrogels. *Tissue Eng. Part A* 17(13–14):1713–1723, 2011.

[23]Kesselman, L. R., S. Shinwary, P. R. Selvaganapathy, and T. Hoare. Synthesis of monodisperse, covalently crosslinked, degradable "smart" microgels using microfluidics. *Small* 8(7):1092–1098, 2012.

[24]Kunz-Schughart, L. A., M. Kreutz, and R. Knuechel. Multicellular spheroids: a three-dimensional *in vitro* culture system to study tumour biology. *Int. J. Exp. Pathol.* 79(1):1–23, 1998.

[25]Lee, G. Y., P. A. Kenny, E. H. Lee, and M. J. Bissell. Three-dimensional culture models of normal and malignant breast epithelial cells. *Nat. Methods* 4(4):359–365, 2007.

[26]Lei, Y., S. Gojgini, J. Lam, and T. Segura. The spreading, migration and proliferation of mouse mesenchymal stem cells cultured inside hyaluronic acid hydrogels. *Biomaterials* 32(1):39–47, 2011.

[27]Lim, F., and A. M. Sun. Microencapsulated islets as bioartificial endocrine pancreas. *Science* 210(4472):908–910, 1980.

[28]Loessner, D., K. S. Stok, M. P. Lutolf, D. W. Hutmacher, J. A. Clements, and S. C. Rizzi. Bioengineered 3D platform to explore cell-ECM interactions and drug resistance of epithelial ovarian cancer cells. *Biomaterials* 31(32):8494–8506, 2010.

[29]Lutolf, M. P., P. M. Gilbert, and H. M. Blau. Designing materials to direct stem-cell fate. *Nature* 462(7272):433–441, 2009.

[30]Lutolf, M. P., and J. A. Hubbell. Synthetic biomaterials as instructive extracellular microenvironments for morphogenesis in tissue engineering. *Nat. Biotechnol.* 23(1):47–55, 2005.

[31]Magley, J., C. Moyers, K. S. Ballard, and S. Tedjarati. Secondary cervical cancer in a patient with chronic lymphocytic leukemia and recurrent chronic lymphocytic leukemia mimicking recurrent cervical dysplasia: a case report. *J. Reprod. Med.* 55(3–4):175–178, 2010.

[32]Metters, A., and J. Hubbell. Network formation and degradation behavior of hydrogels formed by Michael-type addition reactions. *Biomacromolecules* 6(1):290–301, 2005.

[33]Miller, B. E., F. R. Miller, and G. H. Heppner. Factors affecting growth and drug sensitivity of mouse mammary tumor lines in collagen gel cultures. *Cancer Res.* 45(9):4200–4205, 1985.

[34]Panda, P., S. Ali, E. Lo, B. G. Chung, T. A. Hatton, A. Khademhosseini, and P. S. Doyle. Stop-flow lithography to generate cell-laden microgel particles. *Lab Chip* 8(7):1056–1061, 2008.

[35]Phelps, E. A., N. O. Enemchukwu, V. F. Fiore, J. C. Sy, N. Murthy, T. A. Sulchek, T. H. Barker, and A. J. Garcia. Maleimide cross-linked bioactive PEG hydrogel exhibits improved reaction kinetics and cross-linking for cell encapsulation and *in situ* delivery. *Adv. Mater.* 24(1):64–70, 2012.

[36]Qiu, Y., J. J. Lim, L. Scott, Jr., R. C. Adams, H. T. Bui, and J. S. Temenoff. PEG-based hydrogels with tunable degradation characteristics to control delivery of marrow stromal cells for tendon overuse injuries. *Acta Biomater.* 7(3):959–966, 2011.

[37]Raeber, G. P., M. P. Lutolf, and J. A. Hubbell. Molecularly engineered PEG hydrogels: a novel model system for proteolytically mediated cell migration. *Biophys. J.* 89(2):1374–1388, 2005.

[38]Rossow, T., J. A. Heyman, A. J. Ehrlicher, A. Langhoff, D. A. Weitz, R. Haag, and S. Seiffert. Controlled synthesis of cell-laden microgels by radical-free gelation in droplet microfluidics. *J. Am. Chem. Soc.* 134(10):4983–4989, 2012.

[39]Sala, A., P. Hanseler, A. Ranga, M. P. Lutolf, J. Voros, M. Ehrbar, and F. E. Weber. Engineering 3D cell instructive microenvironments by rational assembly of artificial extracellular matrices and cell patterning. *Integr. Biol. (Camb.)* 3(11):1102–1111, 2011.

[40]Salimath, A. S., E. A. Phelps, A. V. Boopathy, P. L. Che, M. Brown, A. J. Garcia, and M. E. Davis. Dual delivery of hepatocyte and vascular endothelial growth factors *via* a protease-degradable hydrogel improves cardiac function in rats. *PLoS ONE* 7(11):e50980, 2012.

[41]Selimovic, S., J. Oh, H. Bae, M. Dokmeci, and A. Khademhosseini. Microscale strategies for generating cell-encapsulating hydrogels. *Polymers (Basel)* 4(3):1554, 2012.

[42]Singh, A., H. Qin, I. Fernandez, J. Wei, J. Lin, L. W. Kwak, and K. Roy. An injectable synthetic immune-priming center mediates efficient T-cell class switching and T-helper 1 response against B cell lymphoma. *J. Controlled Release Off. J. Controlled Release Soc.* 155(2):184–192, 2011.

[43]Singh, A., S. Suri, T. Lee, J. M. Chilton, M. T. Cooke, W. Chen, J. Fu, S. L. Stice, H. Lu, T. C. McDevitt, and A. J. Garcia. Adhesion strength-based, label-free isolation of human pluripotent stem cells. *Nat. Methods* 10(5):438–444, 2013.

[44]Singh, A., S. Suri, and K. Roy. In-situ crosslinking hydrogels for combinatorial delivery of chemokines and siRNA-DNA carrying microparticles to dendritic cells. *Biomaterials* 2009. doi:10.1016/j.biomaterials.2009.06.001.

[45]Suri, S., and C. E. Schmidt. Photopatterned collagen-hyaluronic acid interpenetrating polymer network hydrogels. *Acta Biomater.* 5(7):2385–2397, 2009.

[46]Tomei, A. A., S. Siegert, M. R. Britschgi, S. A. Luther, and M. A. Swartz. Fluid flow regulates stromal cell organization and CCL21 expression in a tissue-engineered lymph node microenvironment. *J. Immunol.* 183(7):4273–4283, 2009.

[47]Weaver, V. M., S. Lelievre, J. N. Lakins, M. A. Chrenek, J. C. Jones, F. Giancotti, Z. Werb, and M. J. Bissell. beta4 integrin-dependent formation of polarized three-dimensional architecture confers resistance to apoptosis in normal and malignant mammary epithelium. *Cancer Cell* 2(3):205–216, 2002.

[48]Weaver, V. M., O. W. Petersen, F. Wang, C. A. Larabell, P. Briand, C. Damsky, and M. J. Bissell. Reversion of the malignant phenotype of human breast cells in three-dimensional culture and *in vivo* by integrin blocking antibodies. *J. Cell Biol.* 137(1):231–245, 1997.